2012

Modeling the Structural Consequences of *BEST1* Missense Mutations

Karina E. Guziewicz
University of Pennsylvania, karinag@vet.upenn.edu

Gustavo D. Aguirre
University of Pennsylvania, gda@vet.upenn.edu

Barbara Zangerl
University of Pennsylvania, bzangerl@vet.upenn.edu

Recommended Citation

Guziewicz, K. E., Aguirre, G. D., & Zangerl, B. (2012). Modeling the Structural Consequences of *BEST1* Missense Mutations. *Retinal Degenerative Diseases: Advances in Experimental Medicine and Biology, 723* 611-618. http://dx.doi.org/10.1007/978-1-4614-0631-0_78

Modeling the Structural Consequences of *BEST1* Missense Mutations

Abstract
Mutations in the bestrophin-1 gene (*BEST1*) are an important cause of inherited retinal disorders. Hitherto, over 100 unique allelic variants have been linked to the human *BEST1* (h*BEST1*), and associated with disease phenotypes, broadly termed as bestrophinopathies. A spontaneous animal model recapitulating *BEST1*-related phenotypes, canine multifocal retinopathy (*cmr*), is caused by mutations in the canine gene ortholog (c*BEST1*). We have recently characterized molecular consequences of *cmr*, demonstrating defective protein trafficking as a result of $G_{161}D$ (*cmr2*) mutation. To further investigate the pathological effects of *BEST1* missense mutations, canine and human peptide fragments derived from the protein sequence have been studied in silico as models for early events in the protein folding. The results showed that $G_{161}D$ as well as $I_{201}T$ substitutions cause severe conformational changes in the structure of bestrophin-1, suggesting protein misfolding as an underlying disease mechanism. The comparative modeling studies expand our insights into *BEST1* pathogenesis.

Keywords
BEST1, bestrophin-1, canine multifocal retinopathy, best vitelliform macular dystrophy, comparative protein modeling, missense mutations

Published in final edited form as:
Adv Exp Med Biol. 2012 ; 723: 611–618. doi:10.1007/978-1-4614-0631-0_78.

Modeling the Structural Consequences of *BEST1* Missense Mutations

Karina E. Guziewicz, **Gustavo D. Aguirre**, and **Barbara Zangerl**
Section of Ophthalmology, Department of Clinical Studies, School of Veterinary Medicine, University of Pennsylvania, Ryan Veterinary Hospital, 3900 Delancey Street, Room 2020, Philadelphia, PA 19104, USA

Barbara Zangerl: bzangerl@vet.upenn.edu

Keywords

BEST1; Bestrophin-1; Canine multifocal retinopathy; Best vitelliform macular dystrophy; Comparative protein modeling; Missense mutations

78.1 Introduction

Bestrophinopathies are a group of inherited retinal disorders primarily caused by point mutations scattered throughout the entire *BEST1* gene. In humans, most of these sequence alterations lead to Best vitelliform macular dystrophy (BVMD), and in dogs cause *cmr*, a retinal phenotype modeling BVMD (Guziewicz et al. 2007, 2011; Zangerl et al. 2010).

The *BEST1* gene product, bestrophin-1 (Best1), is embedded in the basolateral plasma membrane of the RPE, where it functions as a Ca^{2+} dependent anion channel (Marmorstein et al. 2000; Hartzell et al. 2008). Two different topological models of human bestrophin-1 (hBest1) have been proposed. Based on the hydropathy profile analysis, Tsunenari et al. predicted six hydrophobic domains with five transmembrane-spanning segments for the native hBest1 (Tsunenari et al. 2003). Milenkovic et al. proposed a plausible alternative model with four membrane-spanning regions that places residues 95–229 within the cytoplasmic matrix, forming an extensive intracellular loop (Milenkovic et al. 2007). Both models locate the N and C termini on the cytosolic side, and both predict transmembrane domains within the highly evolutionarily conserved N-terminal part of the protein.

Although remarkable progress has been made toward understanding the bestrophin-1 physiology (Sun et al. 2002; Yu et al. 2007; Milenkovic et al. 2007; Qu et al. 2009), our understanding of its complex function and pathological mechanism is still at an early stage. Hitherto, the molecular consequences of altered residues defining three mutational hotspots of the bestrophin-1 molecule (6–30aa, 80–105aa, and 293–312aa) have been the most extensively studied (for review see Hartzell et al. 2008; Boon et al. 2009). These studies established a primary link between *BEST1* mutations and the anion channel malfunction, and provided multiple clues how a particular amino acid substitution may interfere with the protein functionality. In most cases, diminished or absent Cl^- current, altered anion permeability or defective membrane integration in association with bestrophinopathies have been reported (Hartzell et al. 2008; Boon et al. 2009; Xiao et al. 2010). Despite the indisputable advancements made in elucidation of bestrophin-1 pathogenic effects,

Correspondence to: Barbara Zangerl, bzangerl@vet.upenn.edu.

expression and molecular kinetics of mutant transcripts, potential structural consequences, and its impact on the intracellular processing, were either not examined at all or just outlined in few cases (Hartzell et al. 2008; Boon et al. 2009).

We previously described three spontaneous canine bestrophin-1 (cBest1) mutations responsible for *cmr*, an autosomal recessive retinal disorder recognized in numerous dog breeds (Guziewicz et al. 2007; Zangerl et al. 2010). The distinct sequence alterations in c*BEST1* include a nonsense transition ($C_{73}T/R_{25}X$) located in the first coding exon (*cmr1*), a missense substitution ($G_{482}A/G_{161}D$) affecting a conserved glycine residue (*cmr2*), and a frameshift mutation ($C_{1388}del/P_{463}FS$) resulting in a truncated protein shortened by 92 C-terminal aa (*cmr3*) (Guziewicz et al. 2007; Zangerl et al. 2010). Detailed studies on molecular consequences of *cmr1* mutation verified the *BEST1* null phenotype, where $C_{73}T/R_{25}X$ premature stop encodes for a truncated protein not detectable in the homozygous mutant animals or in an in vitro model system (Guziewicz et al. 2011).

In the *cmr2* model, the small (75 Da), neutral, and non-hydrophilic glycine residue at position 161 is replaced by a much larger (133 Da) highly hydrophilic and negatively charged aspartic acid. We speculated that this drastic amino acid change may cause defective intracellular trafficking due to the incorrect folding of the mutant protein that cannot pass the endoplasmic reticulum (ER) quality control system. Indeed, the in-depth characterization of pathogenic effects of $G_{482}A/G_{161}D$ revealed mislocalization of the *cmr2*-bestrophin to the perinuclear space of the cells. Moreover, confocal immuno-fluorescence microscopy analysis indicated co-localization of *cmr2* mutant protein with an ER marker, calnexin (Guziewicz et al. 2011). To further support our hypothesis on *cmr2* protein misfolding and retention in the ER, we used computational approaches to predict the potential structural consequences of the $G_{161}D$ alteration.

78.2 Materials and Methods

78.2.1 Topology Prediction

Topological model of canine bestrophin-1 (NP_001091014) was predicted in silico using Classification and Secondary Structure Prediction of Membrane Proteins SOSUI Server v1.11 (http://bp.nuap.nagoya-u.ac.jp/sosui/; Hirokawa et al. 1998). The model was verified by TopPred II algorithm (Transmembrane Topology Prediction of Membrane Proteins: http://mobyle.pasteur.fr/cgi-bin/portal.py; Claros and von Heijne 1994). Transmembrane segment hydrophobicity scores were calculated according to the GES scale with a cutoff of (−c) 1.8 and (−p) 0.7 (Engelman et al. 1986).

78.2.2 Prediction of Protein Structure

Protein Homology/analogY Recognition Engine (PHYRE Server version 0.2) (http://www.sbg.bio.ic.ac.uk/phyre/; Bennett-Lovsey et al. 2008) was used to perform the secondary fold recognition analysis and tertiary structure prediction for cBest1 (1–296aa) and hBest1 (25–301aa) protein segments. For the putative cBest1 wild-type (WT) structure the estimated precision value (EPV) reached 85% with an e-value of 0.46; for the *cmr2* mutant protein EPV of 75% and e-value of 0.7 was considered. The putative model structures for hBest1 WT (EPV of 80%, e-value of 0.5) and hBest1 $I_{201}T$ mutant (EPV of 85%, e-value of 0.43) were compared to the canine specific predictions. All structures were evaluated on 3D molecule viewer module of the Vector NTI™ 10 software package (Invitrogen).

78.3 Results

78.3.1 Canine Bestrophin-1 Topology

In silico analysis predicted four transmembrane-spanning regions for the native cBest1, orienting the N and C termini to the cytoplasm (Fig. 78.1). According to the SOSUI algorithm, the four most probable transmembrane segments are located at amino acids 32–54, 73–94, 231–253, and 265–287. This model further predicts large, relatively hydrophobic intracellular loop (95–230aa), harboring the G161 residue mutated in *cmr2* (Fig. 78.1). To test whether the location of the transmembrane domains is affected by the *cmr2* mutation, the $G_{161}D$ change was introduced into the protein sequence, and analyzed with the SOSUI algorithm. No effect on the cBest1 topological model was noted with the $G_{161}D$ substitution. The putative cBest1 topology model was verified by TopPred II algorithm (data not shown).

78.3.2 Comparative Protein Modeling

The highly evolutionarily conserved N-terminal part (1–296aa fragment) was used for secondary and tertiary structure prediction of the native cBest1 or the $G_{161}D$ mutant variant (Fig. 78.2). Figure 78.2c–d_1 illustrates the detailed structural environment of the wild-type residues in the native cBest1 in comparison to the *cmr2* mutant model. Replacement of Gly by Asp at position 161 dramatically affects protein structure leading to disrupted intramolecular interactions of neighboring residues (Fig. 78.2b, d–d_1). To assess the relevance of the canine specific findings to human bestrophinopathies, a putative 3D structure for hBest1 (25–301aa fragment) WT or comparable $T_{602}C/I_{201}T$ mutant variant associated with Best disease (Lotery et al. 2000) was predicted by the same algorithm (Fig. 78.3). Significant changes in the $I_{201}T$ mutant protein inducing conformational rearrangements and altered inter-residue interactions are demonstrated in Fig. 78.3d–d_1. Note that only three-dimensional models of EPV ≥ 75% were considered.

78.4 Discussion

Membrane proteins play a crucial role in biological systems as ion channels, pores, and receptors. Understanding their structure and dynamics is essential to expand our knowledge on fundamental aspects of cellular homeostasis. However, only a small fraction of these important proteins has been isolated so far, and the function of most still remains ambiguous. Reasons for this lag include difficulties in expressing such proteins in significant quantities, in isolating and purifying them considering their amphipathic character, and in crystallizing them (http://www.che.udel.edu/cobre/). The recent rapid advances in computer sciences have accelerated their applications to understand complex biological systems, which helped to tackle some of the experimental difficulties. As a consequence, theoretical simulations and computational design methods are now an integral part of biomedical research, becoming an exceptionally useful and powerful means for studying membrane proteins architecture and properties (Casadio et al. 2003). We used two independent computational topology algorithms to assess the putative topology model for cBest1 (Fig. 78.1). Our in silico prediction strongly supports the experimental hBest1 topology model of Milenkovic et al. (2007), which further suggests similar topology for all vertebrate bestrophins. Both models consist of four transmembrane domains in the N-terminus of the protein, separated by a larger intracellular loop, and orienting the C-terminus toward the cytosol (Fig. 78.1; Milenkovic et al. 2007).

The majority of the disease-causing missense mutations identified in humans affect folding or trafficking, rather than specifically affecting protein function (Sanders and Myers 2004). To date, all examined missense changes in the hBest1 were associated with functional consequences, implicating an impaired channel activity. This study demonstrates the

potential structural consequences of $G_{161}D$ (*cmr2*) and comparable hBest1 point mutation, $I_{201}T$, predicted by comparative modeling of the N-terminal part of bestrophin-1. Both analyzed mutations are substitutions replacing a highly evolutionary conserved amino acid with a much bulkier residue (*cmr2*) of different biochemical properties (*cmr2*, $I_{201}T$). Such dramatic changes often affect structure of the encoded protein in the immediate vicinity of the residue, creating electrostatic disturbances and altering the intramolecular inter-actions (Figs. 78.2c_1, d_1 and 78.3c_1, d_1).

The predicted structural rearrangements caused by $G_{161}D$ are in good agreement with previous experiments. Wild type cBest1 is processed in the ER and targeted to the plasma membrane, reflecting normal biogenesis and trafficking of bestrophin-1, but the *cmr2* mutant is retained in the ER (Guziewicz et al. 2011). These data indicate that at least a subset of *BEST1* missense mutations may lead to the protein misassembly, and its build-up in the ER. Since the BVMD and *cmr* are disorders where subretinal deposits accumulate, this mechanism may have an influence on the nature of lesions observed as well as on the disease progression. To support this hypothesis detailed studies are required to further analyze the molecular changes in the early events of the structurally defective bestrophin-1 folding.

Bestrophins are recognized as one of the most mysterious proteins of all known ion channels. To date, Best1 function and kinetics are still not fully understood. Our studies provided new insights into molecular pathology of point mutations associated with *cmr* and Best disease, which is central to the pathogenesis of bestrophinopathies. Additional studies will be required to explore the biochemical and cellular consequences of *BEST1* mutations, and clarify their impact on protein structure with relation to disease onset and progression.

Acknowledgments

This study was supported by The Foundation Fighting Blindness, NEI/NIH grant EY06855, EY17549, The Van Sloun Fund for Canine Genetic Research, Hope for Vision, and P30EY-001583.

References

Bennett-Lovsey RM, Herbert AD, Sternberg MJ, et al. Exploring the extremes of sequence/structure space with ensemble fold recognition in the program Phyre. Proteins. 2008; 70:611–625. [PubMed: 17876813]

Boon CJ, Klevering BJ, Leroy BP, et al. The spectrum of ocular phenotypes caused by mutations in the BEST1 gene. Prog Retin Eye Res. 2009; 28:187–205. [PubMed: 19375515]

Casadio R, Fariselli P, Martelli PL. In silico prediction of the structure of membrane proteins: is it feasible? Brief Bioinform. 2003; 4:341–348. [PubMed: 14725347]

Claros MG, von Heijne G. TopPred II: An Improved Software For Membrane Protein Structure Predictions. Comput Appl Biosci. 1994; 10:685–686. [PubMed: 7704669]

Engelman DM, Steitz TA, Goldman A. Identifying nonpolar transbilayer helices in amino acid sequences of membrane proteins. Annu Rev Biophys Biophys Chem. 1986; 15:321–353. [PubMed: 3521657]

Guziewicz KE, Zangerl B, Lindauer SJ, et al. Bestrophin gene mutations cause canine multifocal retinopathy: a novel animal model for best disease. Invest Ophthalmol Vis Sci. 2007; 48:1959–1967. [PubMed: 17460247]

Guziewicz KE, Slavik J, Lindauer SJP, et al. Molecular consequences of *BEST1* gene mutations in canine multifocal retinopathy predict functional implications for human bestrophinopathies. Invest Ophthalmol Vis Sci. 2011; 52:4497–4505. [PubMed: 21498618]

Hartzell HC, Qu Z, Yu K, et al. Molecular physiology of bestrophins: multifunctional membrane proteins linked to best disease and other retinopathies. Physiol Rev. 2008; 88:639–672. [PubMed: 18391176]

Hirokawa T, Boon-Chieng S, Mitaku S. SOSUI: classification and secondary structure prediction system for membrane proteins. Bioinformatics. 1998; 14:378–379. [PubMed: 9632836]

Lotery AJ, Munier FL, Fishman GA, et al. Allelic variation in the VMD2 gene in best disease and age-related macular degeneration. Invest Ophthalmol Vis Sci. 2000; 41:1291–1296. [PubMed: 10798642]

Marmorstein AD, Marmorstein LY, Rayborn M, et al. Bestrophin, the product of the Best vitelliform macular dystrophy gene (VMD2), localizes to the basolateral plasma membrane of the retinal pigment epithelium. Proc Natl Acad Sci USA. 2000; 97:12758–12763. [PubMed: 11050159]

Milenkovic VM, Rivera A, Horling F, et al. Insertion and topology of normal and mutant bestrophin-1 in the endoplasmic reticulum membrane. J Biol Chem. 2007; 282:1313–1321. [PubMed: 17110374]

Qu Z, Cheng W, Cui Y, et al. Human disease-causing mutations disrupt an N-C-terminal interaction and channel function of bestrophin 1. J Biol Chem. 2009; 284:16473–16481. [PubMed: 19372599]

Sanders CR, Myers JK. Disease-related misassembly of membrane proteins. Annu Rev Biophys Biomol Struct. 2004; 33:25–51. [PubMed: 15139803]

Sun H, Tsunenari T, Yau KW, et al. The vitelliform macular dystrophy protein defines a new family of chloride channels. Proc Natl Acad Sci USA. 2002; 99:4008–4013. [PubMed: 11904445]

Tsunenari T, Sun H, Williams J, et al. Structure-function analysis of the bestrophin family of anion channels. J Biol Chem. 2003; 278:41114–41125. [PubMed: 12907679]

Xiao Q, Hartzell HC, Yu K. Bestrophins and retinopathies. Pflugers Arch. 2010; 460:559–569. [PubMed: 20349192]

Yu K, Qu Z, Cui Y, et al. Chloride channel activity of bestrophin mutants associated with mild or late-onset macular degeneration. Invest Ophthalmol Vis Sci. 2007; 48:4694–4705. [PubMed: 17898294]

Zangerl B, Wickström K, Slavik J, et al. Assessment of canine *BEST1* variations identifies new mutations and established an independent bestrophinopathy model (*cmr3*) in Lapponian Herders. Mol Vis. 2010; 16:2791–2804. [PubMed: 21197113]

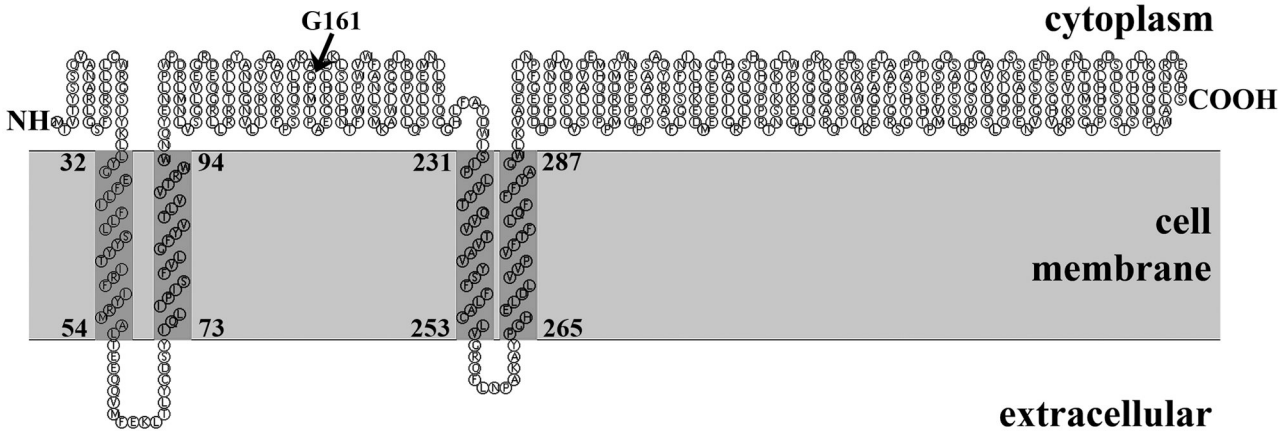

Fig. 78.1.

A representative model of canine bestrophin-1 topology. Two independent computational algorithms (SOSUI, TopPred II) were used to estimate the number of transmembrane domains of the cBest1. Both, the hydropathy index of Kyte and Doolittle and the Goldman, Engelman, and Steitz (GES) hydrophobicity scale, predict four cBest1 transmembrane segments

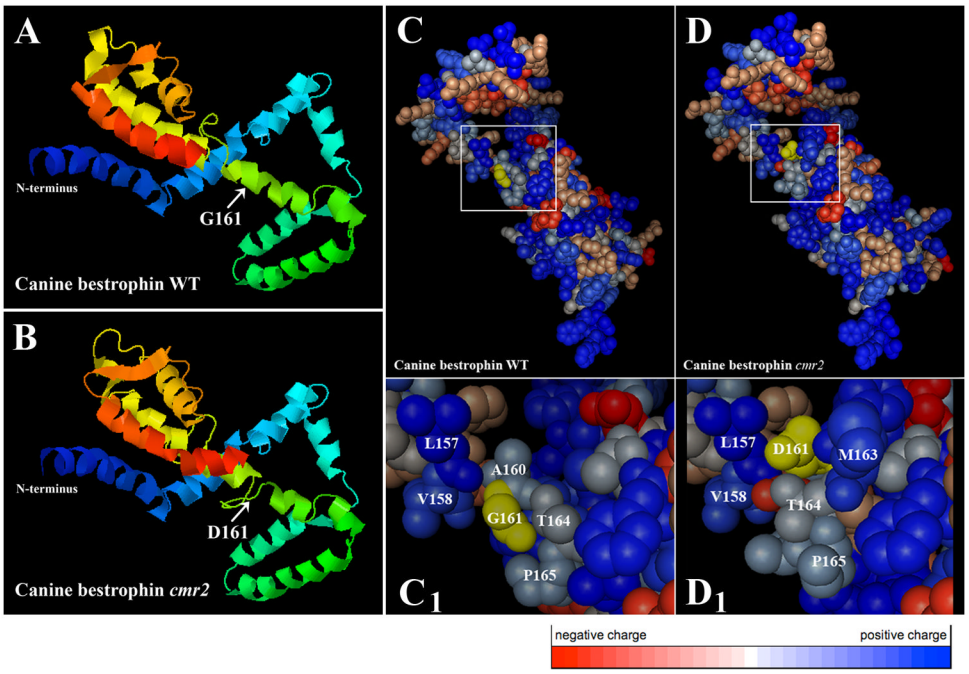

Fig. 78.2.

3D representation of the native and *cmr2* mutant 295aa long N-terminal cBest1 fragment. (**a**, **b**) Overview of the tertiary structure predictions; structural changes caused by $G_{161}D$ substitution are indicated by *arrows*. (**c**, **d**) Detailed structural environment of the wild-type residues in the native cBest1 (**c**) in comparison to the *cmr2* mutant (**d**). Amino acids G161 (WT) and D161 (*cmr2*) are highlighted in *yellow*. (**c_1**, **d_1**) Higher resolution views of the regions denoted by the *white square* in (**c**) and (**d**); Note the significant changes in the amino acid constellations induced by $G_{161}D$ replacement. Color code bar: negatively charged aa are labeled in *red*, whereas positively charged are marked in *blue*

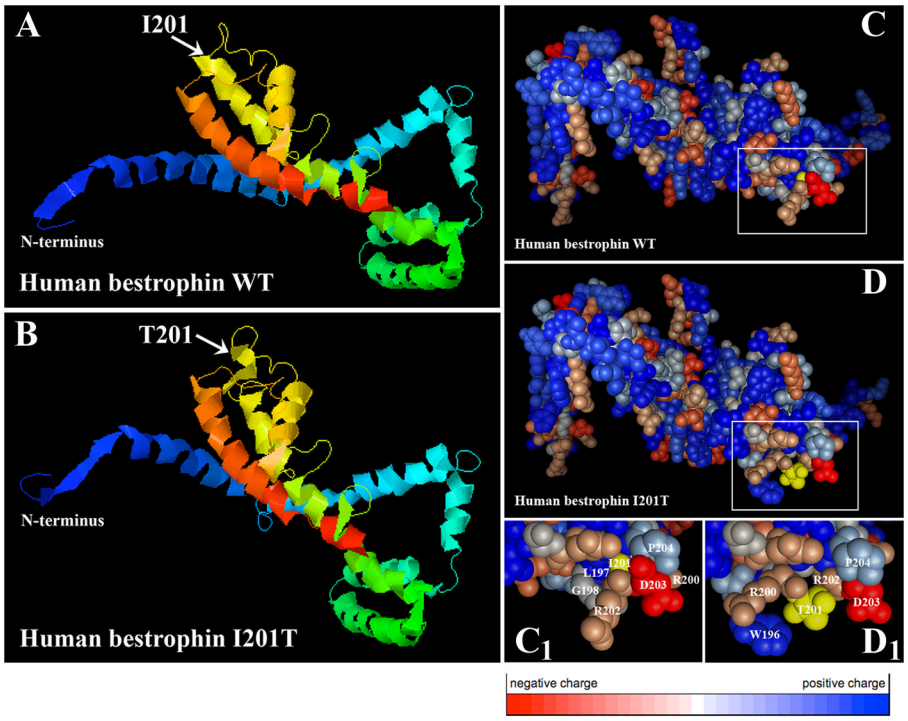

Fig. 78.3.

Computational prediction of 3D models for the native hBest1 and $I_{201}T$ mutant variant (amino acids 25–301). *Arrows* indicate position of I_{201} WT residue (**a**) and T_{201} mutant (**b**). Panels (**c**, **d**) illustrate details of the putative tertiary structure calculated for the native hBest1 (**c**) vs. $I_{201}T$ mutant (**d**); ($\mathbf{c_1}$) and ($\mathbf{d_1}$) show magnifications of the portion denoted by the *white square* in the images (**c**) and (**d**). Wild-type residue I_{201} and mutant T_{201} are highlighted in *yellow*. Note the striking rearrangement of molecular interactions surrounding the T_{201} residue ($\mathbf{d_1}$). Color code bar: negatively charged aa are labeled in *red*, whereas positively charged are marked in *blue*